Cell Host & Microbe
Article

A Tecpr1-Dependent Selective Autophagy Pathway Targets Bacterial Pathogens

Michinaga Ogawa,[1,*] Yuko Yoshikawa,[1] Taira Kobayashi,[1] Hitomi Mimuro,[1] Makoto Fukumatsu,[1] Kotaro Kiga,[1] Zhenzi Piao,[1] Hiroshi Ashida,[1] Mitsutaka Yoshida,[4] Shigeru Kakuta,[3] Tomohiro Koyama,[5] Yoshiyuki Goto,[2] Takahiro Nagatake,[2] Shinya Nagai,[5] Hiroshi Kiyono,[2] Magdalena Kawalec,[6] Jean-Marc Reichhart,[6] and Chihiro Sasakawa[1,7,*]

[1]Division of Bacterial Infection
[2]Division of Mucosal Immunology, Department of Microbiology and Immunology
[3]Center for Experimental Medicine and Systems Biology, Institute of Medical Science
The University of Tokyo, 4-6-1, Shirokanedai, Minato-ku, Tokyo 108-8639, Japan
[4]Division of Ultrastructural Research, BioMedical Research Center, Graduate School of Medicine, Juntendo University, 2-1-1, Hongo, Bunkyo-ku, Tokyo 113-8421, Japan
[5]Nippon Institute for Biological Science, 9-2221-1, Shinmachi, Ome, Tokyo 198-0024, Japan
[6]Institut de Biologie Moléculaire et Cellulaire, Centre National de la Recherche Scientifique Unité Propre de Recherche 9022, Université de Strasbourg, 15, rue Rene Descartes, 67084 Strasbourg Cedex, France
[7]Department of Infectious Disease Control, International Research Center for Infectious Diseases, Institute of Medical Science, The University of Tokyo, 4-6-1, Shirokanedai, Minato-ku, Tokyo 108-8639, Japan
*Correspondence: ogacho@ims.u-tokyo.ac.jp (M.O.), sasakawa@ims.u-tokyo.ac.jp (C.S.)
DOI 10.1016/j.chom.2011.04.010

SUMMARY

Selective autophagy of bacterial pathogens represents a host innate immune mechanism. Selective autophagy has been characterized on the basis of distinct cargo receptors but the mechanisms by which different cargo receptors are targeted for autophagic degradation remain unclear. In this study we identified a highly conserved Tectonin domain-containing protein, Tecpr1, as an Atg5 binding partner that colocalized with Atg5 at *Shigella*-containing phagophores. Tecpr1 activity is necessary for efficient autophagic targeting of bacteria, but has no effect on rapamycin- or starvation-induced canonical autophagy. Tecpr1 interacts with WIPI-2, a yeast Atg18 homolog and PI(3)P-interacting protein required for phagophore formation, and they colocalize to phagophores. Although Tecpr1-deficient mice appear normal, Tecpr1-deficient MEFs were defective for selective autophagy and supported increased intracellular multiplication of *Shigella*. Further, depolarized mitochondria and misfolded protein aggregates accumulated in the Tecpr1-knockout MEFs. Thus, we identify a Tecpr1-dependent pathway as important in targeting bacterial pathogens for selective autophagy.

INTRODUCTION

Selective autophagy has been characterized on the basis of cargo receptors, which are involved in mitophagy, pexophagy, xenophagy, and sequestration of protein aggregates (Deretic, 2010a, 2011; Johansen and Lamark, 2011; Komatsu and Ichimura, 2010), but the mechanisms by which different cargo receptors are targeted for degradation by autophagic pathways is still not completely clear. Xenophagy has been found to play the role of protective cytosolic executioner in the innate immune system, which provides the first line of defense against bacterial intruders (Deretic, 2010a, 2011; Dupont et al., 2009). In the innate immune system, autophagy acts as a cytosolic sensor that recognizes invading bacterial pathogens and their infection events by rapid activation of the autophagic signaling pathway (Ashida et al., 2009; Deretic, 2010a; Huang et al., 2009; Travassos et al., 2010). Selective autophagy is functionally linked to innate immunity in bacterial infection, because selective autophagy plays a key role in sensing bacterial infection in the form of danger-associated molecular patterns (DAMPs), such as those created by membrane pore formation by bacterial cytotoxins and membrane vacuoles damaged by bacterial invasion (Birmingham et al., 2006; Deretic and Levine, 2009; Gutierrez et al., 2007; Viala et al., 2008). In addition to autophagy targeting bacterial infection events, autophagy is able to directly recognize cytosolic bacteria. Several distinct autophagic cargo receptors are involved in recognizing intruding bacterial pathogens. *Salmonella typhimurium* is recognized by three different cargo receptors: p62, NDP52, and diacylglycerol (Cemma et al., 2011; Deretic, 2010a, 2011; Johansen and Lamark, 2011; Shahnazari et al., 2010). Group A *Streptococcus* (GAS) is recognized by NDP52 (Deretic, 2010a) and the invasive processes of *Shigella* and *Listeria monocytogenes*, which create vacuolar membrane remnants, are recognized by the Ub-p62-LC3 pathway (Dupont et al., 2009). The above findings suggest that multiple pathways target bacterial pathogens for selective autophagy, thus playing a vital role in innate defenses against bacterial infection.

Autophagy is initiated by the formation of a phagophore (isolation membrane), a crescent-shaped double membrane that elongates and enfolds a target to form a double-membrane vesicle, the autophagosome (Nakatogawa et al., 2009; Noda and Yoshimori, 2009). There is evidence that autophagosome

formation in mammalian cells is initiated by the formation of a unc-51-like kinase 1 (ULK1) complex and a class III PtdIns 3-kinase (PI3K) complex located at the phagophore and that the formation of these complexes is followed by growth of the phagophore with the aid of additional ATG proteins such as Atg12-Atg5, produced via a Ub-like conjugation reaction between Atg12 and Atg5 (Nakatogawa et al., 2009; Noda and Yoshimori, 2009; Simonsen and Tooze, 2009). Atg12-Atg5 production leads to the formation of an oligomeric complex between the Atg12-Atg5 and Atg16L1 (Mizushima et al., 2003). This complex subsequently acts as an E3 ligase for LC3-II formation at the phagophore (Fujita et al., 2008).

In a previous study we found that a *Shigella* mutant that lacks the *icsB* gene, which encodes the IcsB effector secreted via the type III secretion system (T3SS), is efficiently recognized by Atg5 and Atg5 directly targets the bacterial VirG (IcsA) protein, a virulence-associated outer membrane protein required for bacterial intra- and intercellular spreading (Ashida et al., 2009), which finally leads to the capture of the bacterium by the autophagosome (Ogawa et al., 2005). In the same study we demonstrated that one pole of bacterial surface where Atg5 targets VirG originated the phagophore formation and that this event was independent of ubiquitination. These results suggest that Atg5 serves as a cargo receptor protein in selective autophagy that targets *Shigella* (Ogawa et al., 2005). Because we wanted to learn how the Atg5 targeting VirG could initiate phagophore formation in an Atg5-dependent manner in autophagy, in the present study we attempted to identify Atg5 binding partners in the host. We succeeded in identifying Tecpr1 as an Atg5-interacting protein and found the linkage among VirG, Atg5, Tecpr1, and WIPI-2 in recognizing the *Shigella icsB* mutant in autophagy. We also demonstrated that the WIPI-2-Tecpr1-Atg5 pathway plays an important role in promoting efficient selective autophagy and in targeting protein aggregates and damaged mitochondria.

RESULTS

Tecpr1 Directly Binds to Atg5

We used Atg5 as bait to perform yeast two-hybrid screening of a human brain cDNA library and several truncated protein sequences including DKFZP434B0335 (Tecpr1), FLJ00012 (Atg16L2), MGC23198, Myosin tail domain containing protein, Periphilin 1, and StAR binding protein 1b were identified as a result (Figure S1A, available online). We subsequently performed a GST pull-down assay and selected Atg16L2, MGC23198, and Tecpr1 as Atg5 binding partners (Figure S1B). Because only one of them, the full length of Tecpr1, was detected around a *Shigella* mutant lacking the *icsB* gene (Δ*icsB*) (Figures S1C and S1D), we investigated the tissue distribution of Tecpr1 expression by quantitative RT-PCR. The results showed that although the level of expression of Tecpr1 varied from tissue to tissue, it was almost ubiquitously expressed (Figure S1E). A subsequent GST pull-down assay with purified Atg5 and GST-Tecpr1 showed that they directly bound to each other (Figure 1A). Immunoprecipitation of lysates of 293T/GFP-Tecpr1 or 293T/GFP-Atg5 cells showed that GFP-Tecpr1 interacted with endogenous Atg5 and Atg12-Atg5 (Figure 1B) and that GFP-Atg5 interacted with endogenous Tecpr1 (Figure 1C). Immunoprecipitation of lysates of 293T/GFP-Tecpr1/Atg5-Myc and 293T/GFP-Tecpr1/Atg5^{K130R}-Myc (an Atg12-nonconjugating mutant) (Mizushima et al., 1998) showed that Tecpr1 interacted with Atg5 as well as with Atg12-Atg5 (Figure S1F). Immunoprecipitation of lysates of 293T/GFP-Tecpr1/Atg5-Myc in both the presence and absence of HA-Atg12 showed that Tecpr1 interacted with Atg12-Atg5 but not with Atg12 (Figure S1G). Immunoprecipitation of lysates of 293T/Tcpr1-3Myc/GFP-Atg5, GFP-LC3, GFP-Beclin1, GFP-Vps34, GFPSKD1, and GFP-Rab24 indicated that Tecpr1 predominantly interacted with Atg5 (Figure S1H). Immunoprecipitation of lysates of 293T/Tecpr1-3Myc or Atg5-3Myc showed that, in contrast to Atg5, Tecpr1 did not directly interact with endogenous Atg16L1 (Figure S1I). Finally, immunoprecipitation of lysates of 293T cells showed that endogenous Atg12-Atg5 precipitated with endogenous Tecpr1 and that endogenous Atg16L1 also precipitated because it bound to Atg12-Atg5 (Figure 1D).

Tecpr1 had been reported to be an unknown human ubiquitous protein that contains Dysferlin motifs as well as a Tachylectin-II-like seven-bladed β-propeller and Pleckstrin homology (PH) domain (Figure S1J) (Jeynov et al., 2006). Although the functional role of Tecpr1 in autophagy remains unclear a recent study identified Tecpr1 as one of the binding partners of Atg5 (Behrends et al., 2010). We therefore prepared a series of truncated versions of Tecpr1-3Myc and investigated their ability to interact with the Atg5 in 293T/GFP-Atg5. The results of an immunoprecipitation analysis indicated that the residues 392–719 in Tecpr1 are involved in the direct binding to Atg5 (Figure S1L). A domain analysis revealed that truncated Ub-like domains and the HR domain of Atg5 (Matsushita et al., 2007) have no ability to bind to Tecpr1 and suggested that the full length of Atg5 is necessary for binding to Tecpr1 (Figure S1M). The above findings indicated that the middle portion of Tecpr1 interacts with Atg5 and Atg12-Atg5 and thus that it is indirectly linked to Atg16L1 via its binding to Atg12-Atg5.

Tecpr1-Atg5 Interaction Targets *Shigella* VirG for Selective Autophagy

To characterize the role of Tecpr1 in autophagy, we investigated the involvement of Tecpr1 in bacteria-triggered autophagy by using the *Shigella flexneri* Δ*icsB* mutant (*Shigella* Δ*icsB*), a bacterial strain that is targeted by autophagy (Ogawa et al., 2005). Examination of BHK/GFP-Atg5/Tecpr1-3Myc cells 1 hr after infection with *Shigella* Δ*icsB* revealed that Tecpr1-3Myc had colocalized with GFP-Atg5 around the bacteria (Figure 1F, upper panels). Next, we investigated the spatial relationship between Tecpr1-3Myc, GFP-Atg5, and *Shigella* VirG in BHK/Tecpr1-3Myc/GFP-Atg5 cells 1 hr after infection with *Shigella* Δ*icsB* and found that the Tecpr1-3Myc signals were confined to one pole of the bacterium, whereas VirG and GFP-Atg5 were colocalized (Figure 1F, lower panels). Consistent with these findings, an interaction among GST-VirG and purified Atg5 and MBP-Tecpr1 was detected in a GST pull-down assay (Figure 1E). VirG binding to Atg5 does not require Tecpr1. This suggests that Tecpr1 acts upstream of Atg5 in autophagy of *Shigella*.

To characterize the role of Tecpr1 in autophagy that targets *Shigella*, we investigated the spatial relation to Tecpr1 in the vicinity of the bacterium. When BHK/Tecpr1-3Myc/GFP-LC3 or HeLa/Tecpr1-3Myc/GFP-LC3 cells were infected with *Shigella*

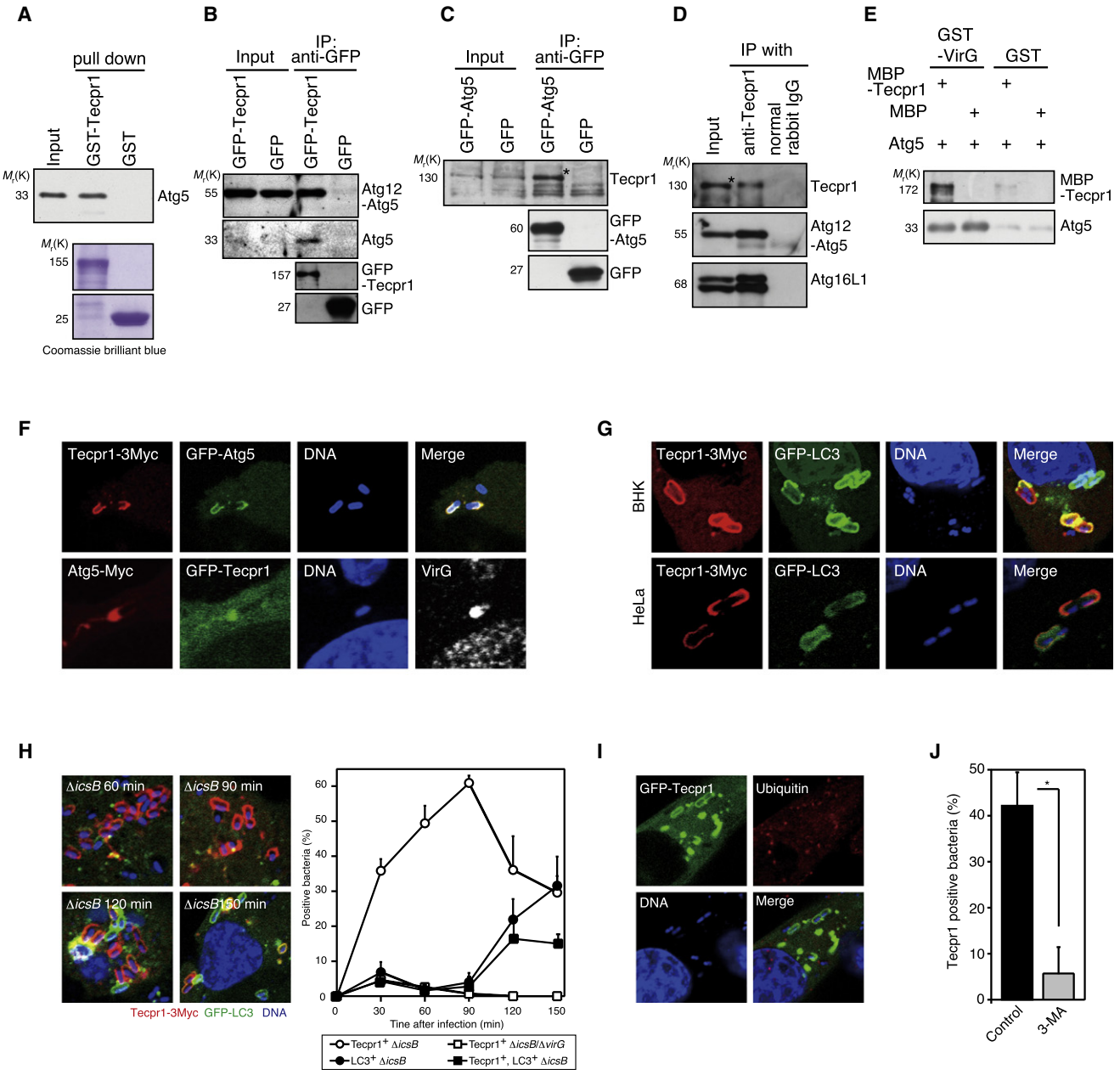

Figure 1. Tecpr1 Associates with Atg5 and Is Involved in *Shigella*-Selective Autophagy

(A) Purified Atg5 was pulled down with GST-Tecpr1 or GST beads and the bound proteins were immunoblotted with an anti-Atg5 antibody.

(B and C) Lysates of 293T cells expressing GFP-Tecpr1, GFP-Atg5, or GFP were immunoprecipitated with an anti-GFP antibody and the bound proteins were immunoblotted with antibodies against (B) Atg5 and GFP or (C) Tecpr1 and GFP. Asterisk indicates major band of Tecpr1.

(D) Lysates of 293T cells were immunoprecipitated with an anti-Tecpr1 antibody and the bound proteins were immunoblotted with antibodies against Tecpr1, Atg5, and Atg16L1. Asterisk indicates major band of Tecpr1.

(E) GST-VirGα1 or GST beads were incubated for 2 hr at 4°C with MBP-Tecpr1 or MBP in the presence of Atg5. The samples were immunoblotted with an antibody against MBP or Atg5.

(F) Colocalization of Tecpr1-3Myc and GFP-Atg5 around *Shigella* Δ*icsB* in BHK cells at 1 hr after infection (upper). Colocalization of Atg5-Myc, GFP-Tecpr1, and VirG at one pole of *Shigella* Δ*icsB* in BHK cells at 1 hr after infection (lower).

(G) Colocalization of Tecpr1-3Myc and GFP-LC3 around *Shigella* Δ*icsB* at 2 hr after infection in the cells indicated.

(H) BHK/Tecpr1-3Myc/GFP-LC3 cells infected with *Shigella* Δ*icsB* (left) or Δ*icsB*/Δ*virG* for the periods indicated were stained with an anti-Myc antibody and DAPI and the number of Tecpr1-3Myc- or GFP-LC3-positive bacteria was counted (right, >500 bacteria, n = 3). Data are the means ± SEM.

(I) BHK/GFP-Tecpr1 cells were infected with *Shigella* Δ*icsB* and 2 hr later they were stained with an FK2 antibody and DAPI.

(J) BHK/Tecpr1-3Myc cells were infected with *Shigella* Δ*icsB* in the presence or absence of 3-methyladenine and the number of Tecpr1-3-Myc-positive bacteria was counted (>500 bacteria, n = 3). Data are the means ± SEM. *p < 0.001.

Δ*icsB* for 2 hr, Tecpr1-3Myc was clearly colocalized with GFP-LC3-positive bacteria, which had been engulfed by autophagosomes (Figure 1G). The number of Tecpr1-positive bacteria in BHK/Tecpr1-3Myc/GFP-LC3 cells infected with Δ*icsB* increased until 90 min, at which point ~60% of the bacteria were Tecpr1-positive but ubiquitin-negative (Figures 1H and 1I). LC3-positive bacteria were detected 120 min postinfection, at which point ~20% of bacteria were LC3-positive and 77.3 ± 12.0% of the LC3-positive bacteria were colocalized with Tecpr1 (Figure 1H). In a previous study we found that VirG on the surface of *Shigella* was a direct target of Atg5 and that a *Shigella* Δ*icsB*/Δ*virG* (deficient IcsB and VirG production by *Shigella*) was not recognized by autophagy (Ogawa et al., 2005). The number of Tecpr1-positive bacteria in BHK/Tecpr1-3Myc/GFP-LC3 cells infected with *Shigella* Δ*icsB*/Δ*virG* (Ogawa et al., 2005) was significantly lower than in *Shigella* Δ*icsB*-infected cells (Figure 1H, right, and Figure S1N). At 2 hr after infection of BHK/Tecpr1-3Myc cells with *Shigella* Δ*icsB* in the presence of 3-methyladenine (3-MA), an autophagy inhibitor whose mechanism of action is inhibition of type III PI3K, far fewer Tecpr1-positive *Shigella* Δ*icsB* were seen (Figure 1J and Figure S1O), implying that type III PI3K is required for Tecpr1 to associate with the phagophore in the targeting of *Shigella* Δ*icsB* by selective autophagy.

Tecpr1 Is Involved in Selective Autophagy

To explore the role of Tecpr1 in selective autophagy, we investigated the involvement of Tecpr1 in targeting GAS and *S. typhimurium*, well-known pathogens that are targets of selective autophagy (Birmingham and Brumell, 2009; Birmingham et al., 2006; Nakagawa et al., 2004; Noda and Yoshimori, 2009; Ogawa et al., 2009). The Tecpr1-3Myc signals in HeLa/Tecpr1-3Myc/GFP-LC3 cells infected with GAS also localized to LC3-positive bacteria (Figure 2A). Similarly, the Tecpr1-3Myc signals in HeLa/Tecpr1-3Myc/GFP-Atg5 cells infected with *S. typhimurium* localized to GFP-Atg5-positive bacteria (Figure 2B) and these Tecpr1-positive bacteria colocalized with Atg16L1, ubiquitin, and LAMP-1 (data not shown).

To investigate whether Tecpr1 is involved in another form of selective autophagy, we stimulated mitophagy in HeLa cells by expressing YFP-PARK2 in the presence of carbonyl cyanide m-chlorophenyl hydrazine (CCCP), an inducer of mitochondrial membrane depolarization (Narendra et al., 2008) and the results showed that the Tecpr1-3Myc signals were strongly colocalized with YFP-PARK2- and LC3-labeled mitochondria (Figures 2C and 2D, upper panels). Furthermore, when GFP-170*, a well-known model substrate for aggresomes (Fu et al., 2005), was transiently expressed in HeLa cells, the Tecpr1-3Myc signals were clearly colocalized at the periphery of LC3-labeled aggresomes composed of GFP-170* (Figures 2C and 2D, lower panels). These results suggested that Tecpr1 was involved in autophagy that selectively targeted large substrates, such as bacteria, depolarized mitochondria, and protein aggregates.

Tecpr1 Is Functionally Involved in Selective Autophagy

To determine whether Tecpr1 participates in promoting canonical autophagy, we examined the localizations of Tecpr1 in BHK/Tecpr1-GFP cells treated with rapamycin, a drug that induces autophagy by inhibiting mTORC1 (Klionsky et al., 2008). Tecpr1-positive puncta were detected after treatment with rapamycin, whereas hardly any Tecpr1-positive puncta were detected after treating the cells with 3-MA (Figure 3A). When HeLa/GFP-Atg5/Tecpr1-3Myc cells were cultured in the presence and absence of rapamycin or vinblastine (inhibitor for autophagosome maturation), Atg5-associated puncta were detected and were colocalized with Tecpr1-3Myc (Figure 3B). When HeLa/GFP-Tecpr1 cells were cultured in the presence or absence of rapamycin or vinblastine, GFP-Tecpr1 signals were detected and were associated with vacuolar structures that stained positive with monodansylcadaverine (MDC), a marker of autophagosomes and lysosomes (Figure 3C). In addition, in HeLa/Tecpr1-3Myc/GFP-LC3 cells cultured in the presence or absence of rapamycin or vinblastine, Tecpr1-positive puncta were also detected and were colocalized with LC3-positive puncta (Figure 3D). Taken together, these findings suggested that Tecpr1 is localized at autophagosomes.

To determine how Tecpr1 is involved in autophagy, we performed knockdown experiments with Tecpr1 siRNA. After knocking down Tecpr1 in MEF/GFP-LC3 cells (Figure S2A), hardly any LC3-positive puncta were detected after rapamycin treatment (Figures 4A and 4B). The LC3-II/LC3-I ratio in Tecpr1-knockdown HeLa/GFP-LC3 or 293T cells (Figure S2A) cultured in DMEM in the presence or absence of rapamycin or EBSS was slightly lower than in the siLuc control cells (Figures 4C and 4D and Figures S2B and S2C). Even when autophagosome maturation was inhibited by treatment with vinblastine or bafilomycin A1, the slight decrease in LC3-II/LC3-I ratio in the Tecpr1 knockdown HeLa/GFP-LC3 or 293T cells was sustained (Figures S2B and S2C). Because the Atg12-Atg5 conjugate acts like an E3-like enzyme and catalyzes the conversion of LC3-I to LC3-II (Fujita et al., 2008), we investigated the effect of Tecpr1 knockdown on the levels of Atg12-Atg5 in 293T and HeLa/GFP-Atg5 cells. Tecpr1 knockdown resulted in a great decrease in the level of Atg12-Atg5 and an increase in the level of unconjugated Atg5 (Figures 4E and 4F). We then examined the effect of Tecpr1 on formation of the Atg12-Atg5 conjugate by means of an in vitro reconstitution assay and found that Atg12-Atg5 conjugation was greatly promoted by Tecpr1 (Figure 4G). These results suggest that the role of Tecpr1 in canonical autophagy is not substantial, but that Tecpr1 may play a role in selective autophagy in which urgent, massive Atg12-Atg5 formation is needed.

Indeed, electron microscopic analysis revealed the presence of many more highly electron-dense aggregate-like bodies and multivesicular bodies (MVBs) in Tecpr1 knockdown cells than in the siLuc control cells (Figure 4H). Because selective autophagy for large substrates such as toxic aggresomes needs rapid and bulky membrane elongation by Atg12-Atg5, these findings suggested functional involvement of Tecpr1 in selective autophagy for large substrates via promoting Atg12-Atg5 reaction.

We examined the effect of Tecpr1 knockdown on autophagy-targeting bacteria. The number of LC3-positive bacteria in Tecpr1 knockdown HeLa/GFP-LC3 cells infected with *Shigella* Δ*icsB* for 2 hr was significantly lower than in the control cells (Figures 5A and 5B). The number of intracellular *Shigella* Δ*icsB* in Tecpr1 knockdown HeLa cells was significantly higher than in the control cells (Figure 5C). Similarly, the number of LC3-positive bacteria

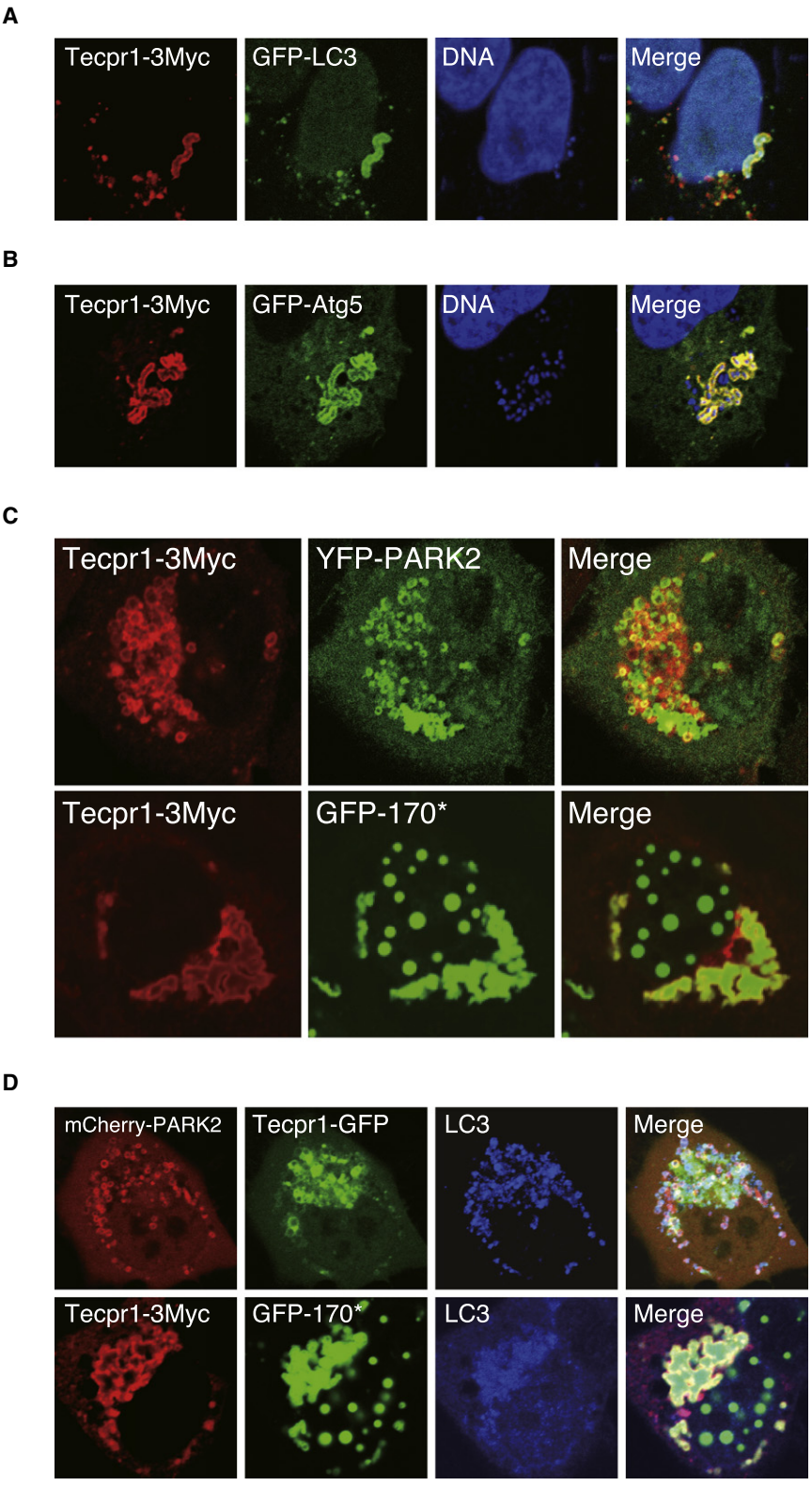

Figure 2. Tecpr1 Is Involved in Selective Autophagy-Targeting Pathogens, Aggresomes, and Mitochondria

(A) HeLa/Tecpr1-3Myc/GFP-LC3 cells were infected with GAS and 2 hr later they were stained with an anti-Myc antibody and DAPI.

(B) HeLa/Tecpr1-3Myc/GFP-Atg5 cells were infected with *S. typhimurium* and 1 hr later they were stained with an anti-Myc antibody and DAPI.

(C) HeLa/Tecpr1-3Myc/YFP-PARK2 cells treated with 10 μM CCCP for 4 hr were stained with an anti-Myc antibody (upper panels). HeLa/Tecpr1-3Myc/GFP-170* cells were stained with an anti-Myc antibody (lower panels).

(D) HeLa/Tecpr1-GFP/mCherry-PARK2 cells treated with 10 μM CCCP for 4 hr were stained with an anti-LC3 antibody (upper panels). HeLa/Tecpr1-3Myc/GFP-170* cells were stained with an anti-LC3 antibody (lower panels).

in Tecpr1 knockdown HeLa/GFP-LC3 cells infected with GAS for 2 hr was much lower than in the control cells (Figures 5D and 5E).

Tecpr1-WIPI-2 Interaction Is Involved in Selective Autophagy

Although the Tecpr1-positive membrane structures enclosing *Shigella* Δ*icsB* in the wild-type MEFs are closely attached, those structures in the Atg5-knockout MEFs appeared to be incomplete, but Tecpr1 remained anchored on the phagophore membrane around bacteria in the absence of Atg5 (Figure 6A). We attempted to identify the factor(s) that harnesses Tecpr1 to the phagophore membrane even in the absence of Atg5. Recent studies have reported finding that Tecpr1 interacts with Atg5, TRS85, TRAPP4, and TTC15 (Behrends et al., 2010) and that Rab1, a TRS85 GEF target, is localized at autophagosomes around *Salmonella* (Huang et al., 2011), suggesting that Tecpr1 has multiple binding partners, although the functional significance of interaction between Tecpr1 and its binding partners remains unclear. Then we examined the localization of the above putative Tecpr1 binding partners to phagophore membrane around bacteria in BHK/Tecpr1-3Myc cells infected with *Shigella* Δ*icsB*, but none of the binding partners were colocalized around the bacteria (Figure S3A). Because type III PI3K was shown to be required for the proper localization of Tecpr1 around *Shigella* Δ*icsB* (Figure 1J and Figure S1O), we postulated the participation of a PI(3)P-dependent Tecpr1-targeting pathway in phagophore formation and investigated the ability of Tecpr1 to interact with the type III PI3K-complex-related proteins Atg14, Beclin1, Rubicon, Vps15, and Vps34 (Noda et al., 2010; Simonsen and Tooze, 2009). Rubicon showed slight ability to bind to Tecpr1, but the

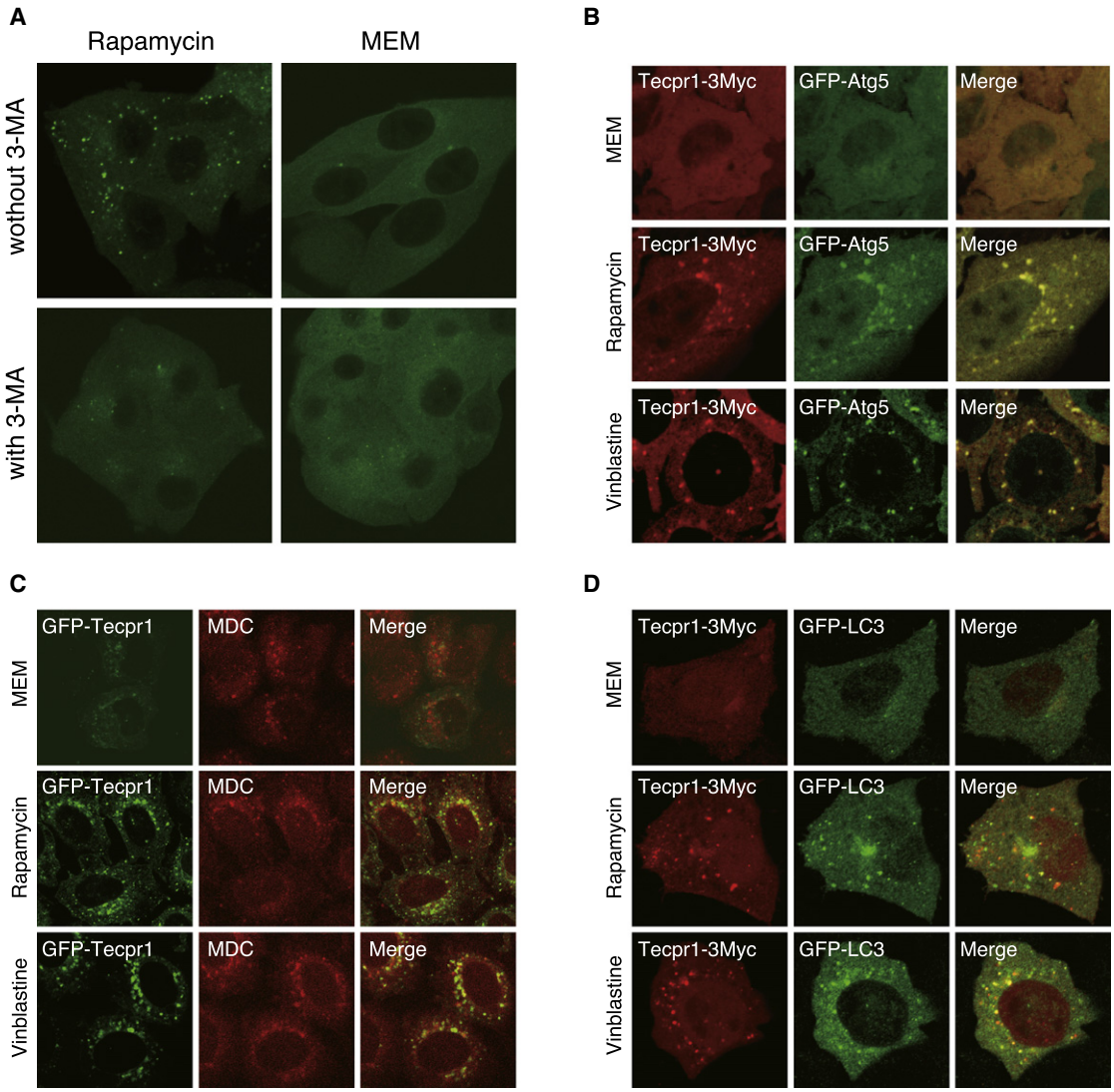

Figure 3. Tecpr1 Is Colocalized with Autophagosomes in Canonical Autophagy

(A) BHK/Tecpr1-GFP cells were cultured for 2 hr in MEM and FCS or MEM and FCS containing rapamycin in the presence or absence of 3-methyladenine.

(B) HeLa/Tecpr1-3Myc/GFP-Atg5 cells cultured in MEM and FCS in the presence or absence of the autophagy inducers indicated were stained with an anti-Myc antibody.

(C) HeLa/GFP-Tecpr1 cells cultured in MEM and FCS in the presence or absence of the autophagy inducers indicated were stained with MDC.

(D) MEF/Tecpr1-3Myc/GFP-LC3 cells cultured in MEM and FCS in the presence or absence of the autophagy inducers indicated were stained with an anti-Myc antibody.

ability of the other type III PI3K-complex-related proteins to bind to Tecpr1 was poor (Figure S3B). Although Tecpr1 contains FRRG motifs, which are the lipid binding motifs in WIPI family proteins (Polson et al., 2010), MBP-Tecpr1 showed no ability to interact with PI(3)P beads (Figure S3C). Because Low et al. showed that Tecpr1 contains a lectin-like domain that is involved in binding to sugars, especially galactose and acetylated glucose (Low et al., 2009, 2010; Saito et al., 1995), in an in silico domain analysis, we assessed the ability of Tecpr1 to bind to a lactose- or GlcNAc-immobilized gel, but the results showed that GFP-Tecpr1 did not bind to either immobilized gel (Figures S3D and S3E). We subsequently investigated the localization of WIPI-2, a yeast Atg18 homolog PI(3)P-interacting protein required for phagophore formation and elongation (Polson et al., 2010), on the Tecpr1-positive autophagosomes in *Shigella* Δ*icsB*-infected cells. When BHK/Tecpr1-3Myc/WIPI-2-GFP cells were infected with Δ*icsB*, although WIPI-2 signals were occasionally observed as puncta on phagophores engulfing the bacteria, the WIPI-2 and Tecpr1 signals were colocalized around the bacteria (Figure 6B). When lysates of 293T/2HA-WIPI-2/Tecpr1-GFP cells were immunoprecipitated with an anti-GFP antibody, Tecpr1 coprecipitated with WIPI-2 (Figure 6C). A domain analysis revealed that the TECPR domain located in the C-terminal portion of Tecpr1 was involved in the binding to WIPI-2 (Figure S3F). When a WIPI-2 FKKG mutant lacking PI(3)P binding capacity was used in an immunoprecipitation assay for Tecpr1-GFP, the WIPI-2 FKKG mutant was able to

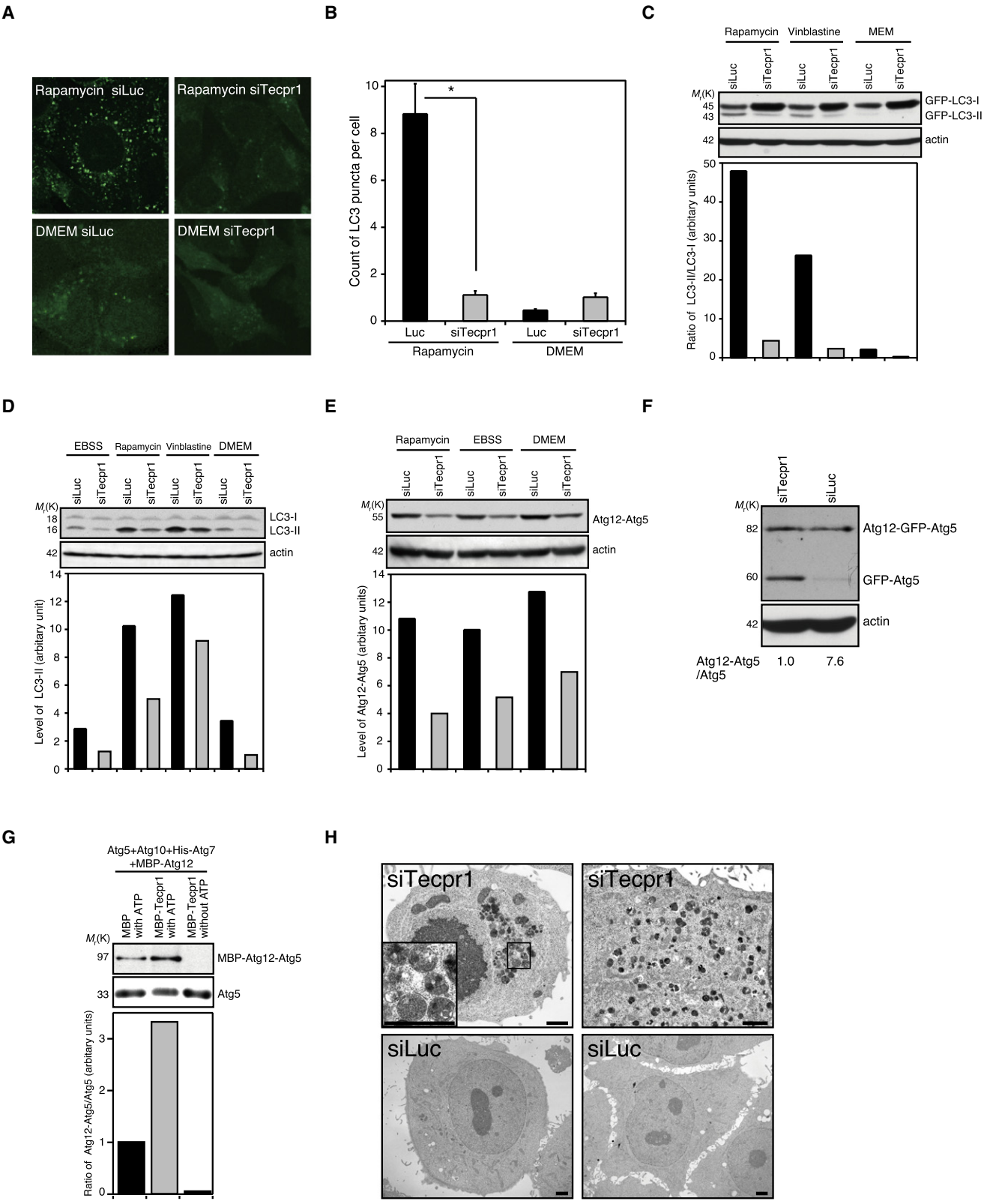

Figure 4. Function Analysis of Tecpr1 in Canonical Autophagy

(A) MEF/GFP-LC3 cells treated with the siRNAs indicated were cultured in the presence or absence of rapamycin (left) and (B) the number of autophagic puncta was counted (right, >300 cells, n = 3). Data are the means ± SEM. *p < 0.001.

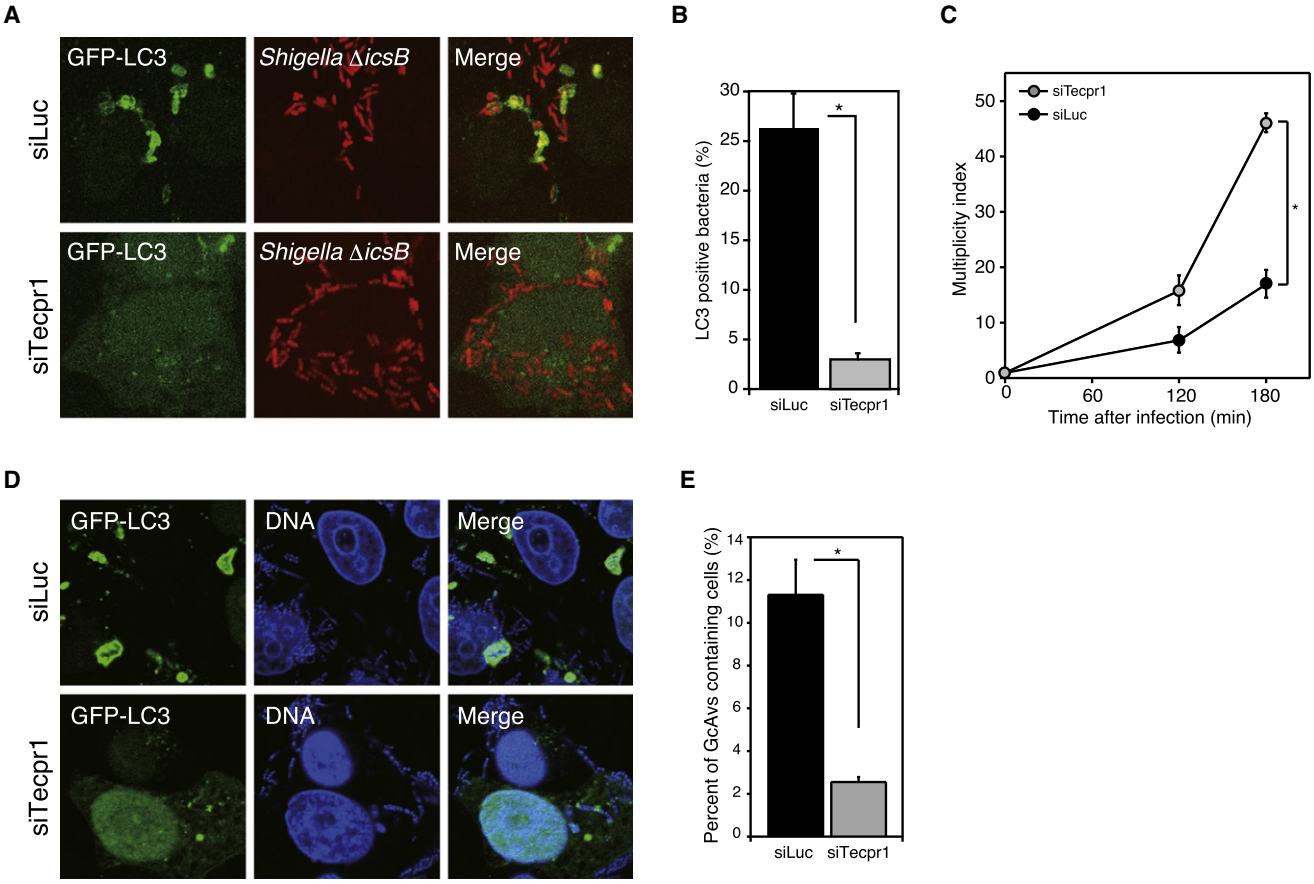

Figure 5. Function Analysis of Tecpr1 in Selective Autophagy of *Shigella*

(A and B) HeLa/GFP-LC3 cells treated with the siRNAs indicated were infected with *Shigella* Δ*icsB*/pBR-DsRed and 2 hr later they were stained with anti-*Shigella* LPS antibody (A) and the number of GFP-LC3-positive bacteria was counted (>500 bacteria, n = 3) (B). Data are the means ± SEM. *p < 0.001.

(C) HeLa cells treated with the siRNAs indicated were infected with *Shigella* Δ*icsB* and intracellular bacterial growth was determined by cfu (n = 3). Data are the means ± SEM. *p < 0.001.

(D) HeLa/GFP-LC3 cells were treated with the siRNAs indicated and 2 hr after infecting them with GAS they were stained with DAPI.

(E) The number of GAS-containing autophagosome-like vacuole (GcAVs)-positive cells was counted (>300 cells, n = 3). Data are the means ± SEM. *p < 0.001.

interact with Tecpr1-GFP as strongly as wild-type WIPI-2, suggesting that the PI(3)P binding activity of WIPI-2 is not required for the interaction with Tecpr1 (Figure S3G). When WIPI-2 knockdown HeLa/Tecpr1-GFP cells (Figure S3H) were infected with *Shigella* Δ*icsB*, the number of Tecpr1-positive bacteria was one-third of the number in the control cells (Figure 6D). As reported by Polson et al. (Polson et al., 2010), in WIPI-2 knockdown HeLa/Atg5-Myc or 293T cells, the autophagic activities determined by the levels of Atg12-Atg5 and LC3-II were lower than in the siLuc control cells (Figures S3I and S3J). Based on the above findings we concluded that the PI(3)P associated with phagophores recruited WIPI-2, Tecpr1, and Atg5, in that order, and that the interaction between Tecpr1 and WIPI-2 is functionally important to promoting autophagy that targets bacteria (Figure S5).

Tecpr1-Knockout MEFs Demonstrate the Importance of Tecpr1 for Selective Autophagy

To confirm the in vivo role of Tecpr1 in selective autophagy and clarify how Tecpr1 is involved in autophagic events, we generated Tecpr1 knockout (Tecpr1$^{-/-}$) mice by a gene-targeting method (Figures S4A–S4E). Tecpr1$^{-/-}$ mice were born healthy, in the expected Mendelian ratio, and with no gross phenotypic

(C and D) HeLa/GFP-LC3 (C) or 293T cells (D) treated with the siRNAs indicated were cultured under the conditions indicated. Lysates were subjected to immunoblotting with anti-GFP (C) or anti-LC3 (D) antibodies. The LC3-II/LC3-I ratios were quantified.

(E) 293T cells treated with the siRNAs indicated were cultured under the conditions indicated. Lysates were subjected to immunoblotting with anti-Atg5 antibody. The Atg12-Atg5 levels were quantified.

(F) Lysates of HeLa/GFP-Atg5 cells treated with the siRNAs indicated were subjected to immunoblotting with anti-GFP and the Atg12-Atg5/Atg5 ratios were quantified.

(G) An in vitro Atg12-Atg5 reconstitution assay was performed in the presence or absence of MBP-Tecpr1. Samples were subjected to immunoblotting with antibodies against MBP or Atg5. The Atg12-Atg5/Atg5 levels were quantified.

(H) HeLa cells treated with the siRNAs indicated were examined by electron microscopy. Scale bars = 2 μm.

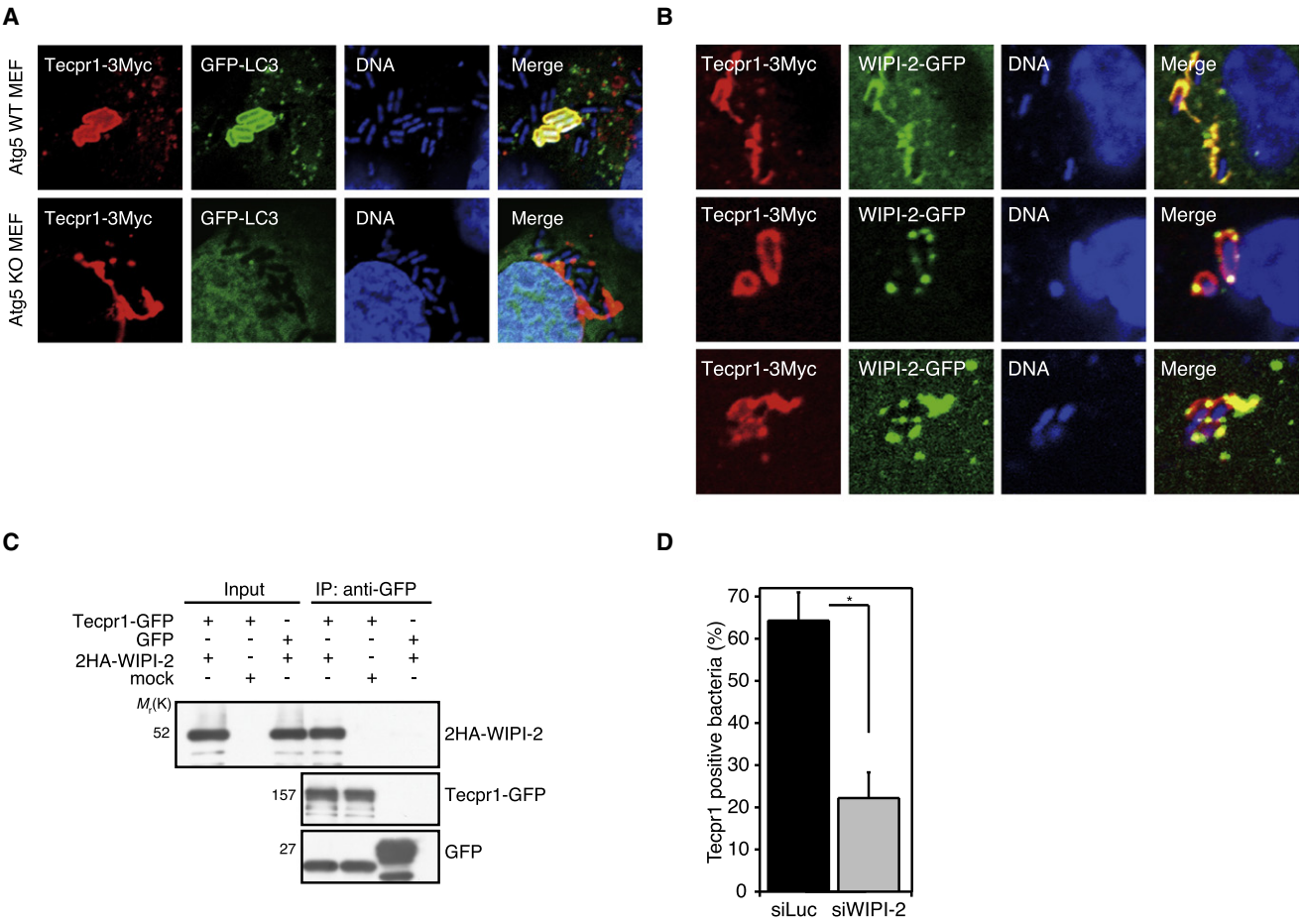

Figure 6. Interaction between Tecpr1 and WIPI-2 Is Involved in the Proper Localization of Tecpr1

(A) Atg5$^{+/+}$ or Atg5$^{-/-}$ MEFs expressing Tecpr1-3Myc and GFP-LC3 were infected with *Shigella* Δ*icsB* and 2 hr later they were stained with an anti-Myc antibody and DAPI.

(B) BHK/Tecpr1-3Myc/WIPI-2-GFP cells were infected with *Shigella* Δ*icsB* and 90 min later they were stained with an anti-Myc antibody and DAPI.

(C) Lysates of 293T/2HA-WIPI-2 cells expressing GFP-Tecpr1 or GFP were immunoprecipitated with an anti-GFP antibody and the bound proteins were immunoblotted with antibody against HA or GFP.

(D) HeLa/Tecpr1-GFP cells treated with the siRNAs indicated were infected with *Shigella* Δ*icsB*/pBR-DsRed and 90 min later the number of Tecpr1-GFP-positive bacteria was counted (>500 bacteria, n = 3). Data are the means ± SEM. *p < 0.001.

abnormalities and they survived during neonatal starvation, suggesting that Tecpr1 activity is dispensable for maintaining basal autophagy. Although slight differences in the levels of LC3-II, p62, and Atg12-Atg5 between Tecpr1$^{-/-}$ MEFs and Tecpr1$^{+/+}$ MEFs were seen under full-nutrient conditions (Figures S4F–S4I), no differences between Tecpr1$^{-/-}$ and Tecpr1$^{+/+}$ MEFs were detected when treated with rapamycin (Figures S4F–S4I), suggesting that Tecpr1 does not play a substantial role in promoting canonical autophagy. There was no difference in Atg16L1 levels between Tecpr1$^{-/-}$ and Tecpr1$^{+/+}$ MEFs, suggesting that the Atg12-Atg5-Atg16L1 complex is stable in the absence of Tecpr1 (Figures S4H and S4I). The LC3-II levels in Tecpr1$^{-/-}$ and Tecpr1$^{+/+}$ MEFs increased similarly in the presence of bafilomycin A1 (Figures S4F and S4G), suggesting that autophagic flux was normal in the Tecpr1$^{-/-}$ MEFs (Klionsky et al., 2008). Electron microscopic analysis of the Tecpr1$^{-/-}$ MEFs revealed that many of them contained aggregates and MVBs (Figure 7A) and the presence of MVBs seemed to mirror the accumulation of anti-lysobisphosphatidic acid (LBPA) antibody-stained puncta (Figure 7B). The accumulation of MVBs in Tecpr1$^{-/-}$ MEFs was reminiscent of the accumulation of MVBs in Tecpr1 knockdown HeLa cells (Figure 4H).

Aggregates of ubiquitinated proteins are a specific substrate for selective autophagy (Johansen and Lamark, 2011; Komatsu and Ichimura, 2010). Acute aggregate formation can be induced by treatment with puromycin, a translational inhibitor that induces accumulation of misfolded proteins (Huang et al., 2011). To examine the ability to clear aggregate bodies in Tecpr1$^{-/-}$ MEFs, we performed an aggregate clearance assay. After pulsing each MEF with puromycin for 4 hr, the cells were washed to remove the puromycin and incubated for 4 or 6 hr more and the number of aggregates were counted. Consistent with the results of the electron microscopic analysis (Figure 7A), clearance of the aggregates in Tecpr1$^{-/-}$ MEFs was reduced in comparison with the Tecpr1$^{+/+}$ MEFs (Figures 7C and 7D). Because recent studies have indicated that autophagy and mitochondrial morphology

interact reciprocally (Radoshevich et al., 2010; Singh et al., 2010), we investigated the effect of Tecpr1 knockout on the accumulation of depolarized mitochondria. As shown in Figure 7E, the tangled and condensed mitochondria, which stained positive with an anti-mtHSP70 antibody, in Tecpr1$^{-/-}$ MEFs were stronger than in Tecpr1$^{+/+}$ MEFs, although some scattered mitochondria were detected in the Tecpr1$^{+/+}$ MEFs (Figure 7E and Figure S4J). The mtHSP70 level in the Tecpr1$^{-/-}$ MEFs was 2.3-fold higher than in the Tecpr1$^{+/+}$ MEFs (Figure 7E).

Accumulation of depolarizing mitochondria has been reported in autophagy-deficient mammalian cells (Tal et al., 2009). We therefore investigated the effect of Tecpr1 activity on the accumulation of depolarizing mitochondria in Atg5$^{-/-}$, Atg5$^{+/+}$, Tecpr1$^{-/-}$, and Tecpr1$^{+/+}$ MEFs. More than 99% of Atg5$^{+/+}$ and Tecpr1$^{+/+}$ MEFs treated with CCCP as a control were positive for accumulation of depolarized mitochondria (Figure S4K). As reported by Tal et al., the number of cells with accumulation of depolarized mitochondria in Atg5$^{-/-}$ MEFs (27.9%) was higher than in Atg5$^{+/+}$ MEFs (16.3%) (Figure S4K). Similarly, the number of cells with accumulation of depolarized mitochondria in Tecpr1$^{-/-}$ MEFs (28.7%) was higher than in Tecpr1$^{+/+}$ MEFs (15.0%) (Figure S4K). The FACS analyses provided further evidence that Tecpr1 is involved in the selective autophagic pathway.

Finally, we confirmed the effect of Tecpr1 knockout on autophagy that targets bacteria. Two hours after Tecpr1$^{-/-}$ or Tecpr1$^{+/+}$ MEFs stably expressing GFP-LC3 were infected with *Shigella* Δ*icsB*, the number of LC3-positive bacteria in Tecpr1$^{-/-}$ MEFs was much lower than in the Tecpr1$^{+/+}$ MEFs (Figure 7F). However, many more *Shigella* Δ*icsB* survived in Tecpr1$^{-/-}$ MEFs than in Tecpr1$^{+/+}$ MEFs (Figure 7G), a finding that was consistent with the results observed in Tecpr1 knockdown HeLa cells (Figure 5C).

DISCUSSION

In this study we identified Tecpr1 as a binding partner of Atg5 and WIPI-2 (yeast Atg18 homolog in mammals) and found evidence that supports the notion that Tecpr1 plays an important role in selective autophagy, such as the autophagy that selectively targets bacterial pathogens, damaged mitochondria, and protein aggregates. In this study we found the following: (1) Tecpr1 signals were localized to Atg5- and LC3-positive but Ub-negative autophagosomes that had surrounded *Shigella* Δ*icsB*, (2) Tecpr1 localized at autophagosomes that targeted GAS and *S. typhimurium*, (3) Tecpr1 localized at depolarized mitochondria and misfolded protein aggregates, (4) Tecpr1 knockdown resulted in an increase in the number of *Shigella* Δ*icsB* that survived intracellularly and Atg12-Atg5 conjugation and protein aggregate clearance decreased, (5) WIPI-2 was necessary for proper localization of Tecpr1 to phagophore in the vicinity of *Shigella* Δ*icsB*, (6) Tecpr1$^{-/-}$ mice were born and the canonical autophagy in the Tecpr1$^{-/-}$ MEFs was sustained, but MVBs and depolarized mitochondria accumulated in the Tecpr1$^{-/-}$ MEFs, and (7) the more *Shigella* Δ*icsB* survived in the Tecpr1$^{-/-}$ MEFs. Taken together, these findings strongly indicated that Tecpr1 plays a vital role in promoting selective autophagy.

Tecpr1 is a highly conserved protein among multicellular organisms and has been identified in species ranging from *Caenorhabditis elegans* to humans. Tecpr1 contains several distinctive domains, including two DysF domains, nine Tectonin repeats (TECPR) domains, and a unique PH domain in the middle of the protein, as well as a characteristic β-propeller structure (Figure S1J) (Jeynov et al., 2006; Low et al., 2009, 2010; Patel et al., 2008; Saito et al., 1995). Tecpr1 has an ortholog, Tecpr2, that lacks the central PH domain; however, our findings indicate that Tecpr2 does not play a role in targeting *Shigella* by autophagy or have the ability to interact with Atg5 (Figure S1K and data not shown). Tecpr1 presumably interacts with multiple host factors, the same as some other proteins that contain a β-propeller structure including tryptophan-aspartate repeat (WD-repeat). The DysF domain is composed of DysF-N and DysF-C and is conserved in human dysferlin, myoferlin, and fer-1, in yeast YIPex23, and in *Drosophila melanogaster* CG6468, all of which have been shown to have some ability to interact with caveolin-3 (Patel et al., 2008) and thus are involved in membrane repair. Intriguingly, the TECPR domain is also found in *Tachypleus tridentatus* (horseshoe crab) L-6 lectin, Tachylectin-2, and galactose binding protein (GBP) (Low et al., 2009, 2010; Saito et al., 1995) and in the Tectonin of the slime mold *Hysayum polycepalum*. Furthermore, Tecpr1 has been shown to have some ability to interact with the sugar moiety of lipopolysaccharide and with acetylated sugar chains (Low et al., 2009). Low et al. showed that *T. tridentatus* GBP has the ability to interact with carcinolectin-5 (CL5) of the horseshoe crab and in a yeast two-hybrid assay they demonstrated that Tecpr1 can also interact with ficolin of humans, the homolog of horseshoe crab CL5, neutrophil cytosol factor 1 (NCF1), Srk-like adaptor 2 (SLA2), and ubiquitin-specific-processing protease (CYLD) (Low et al., 2010). Furthermore, Behrends et al. recently showed by a bioinformatics approach that Tecpr1 has the ability to interact with Atg5, TTC15, TRAPP4, and TRS85, although the biological significance of the interaction between Tecpr1 and these proteins remains unclear (Behrends et al., 2010). The results of these studies taken together suggest that Tecpr1 may be a versatile protein that is involved not only in selective autophagy but also in sensing, if only indirectly, microbial components and some lectins involved in host innate immunity.

We assume that Tecpr1 indirectly associates with phagophores through the interaction between the middle portion of Tecpr1 and Atg12-Atg5-Atg16. Although the affinity of Atg16 for Atg12-Atg5 is much stronger than for Atg5 (Mizushima et al., 2003), the affinity of Tecpr1 for Atg12-Atg5 and Atg5 appeared to be similar based on the results of an immunoprecipitation assay (Figure S1F). Importantly, we did not detect localization of Rab1, TRAPP4, TRS85c, or TTC15 (TRAPIII family proteins) with autophagosomes enclosing *Shigella* Δ*icsB*, suggesting that none of these Tecpr1 binding partners except Atg5 have any appreciable role in the WIPI-2-Tecpr1-Atg5 pathway.

In the present study, we identified WIPI-2 as a Tecpr1 binding partner, and we demonstrated that WIPI-2 is a functionally important protein for selective autophagy that targets bacteria. A recent study has indicated that WIPI-2 participates in triggering the formation and elongation of phagophores (Polson et al., 2010). Our study demonstrated the following: (1) Tecpr1 bound to WIPI-2 in an immunoprecipitation assay, (2) the TECPR domain in the C-terminal portion of Tecpr1 is involved in WIPI-2

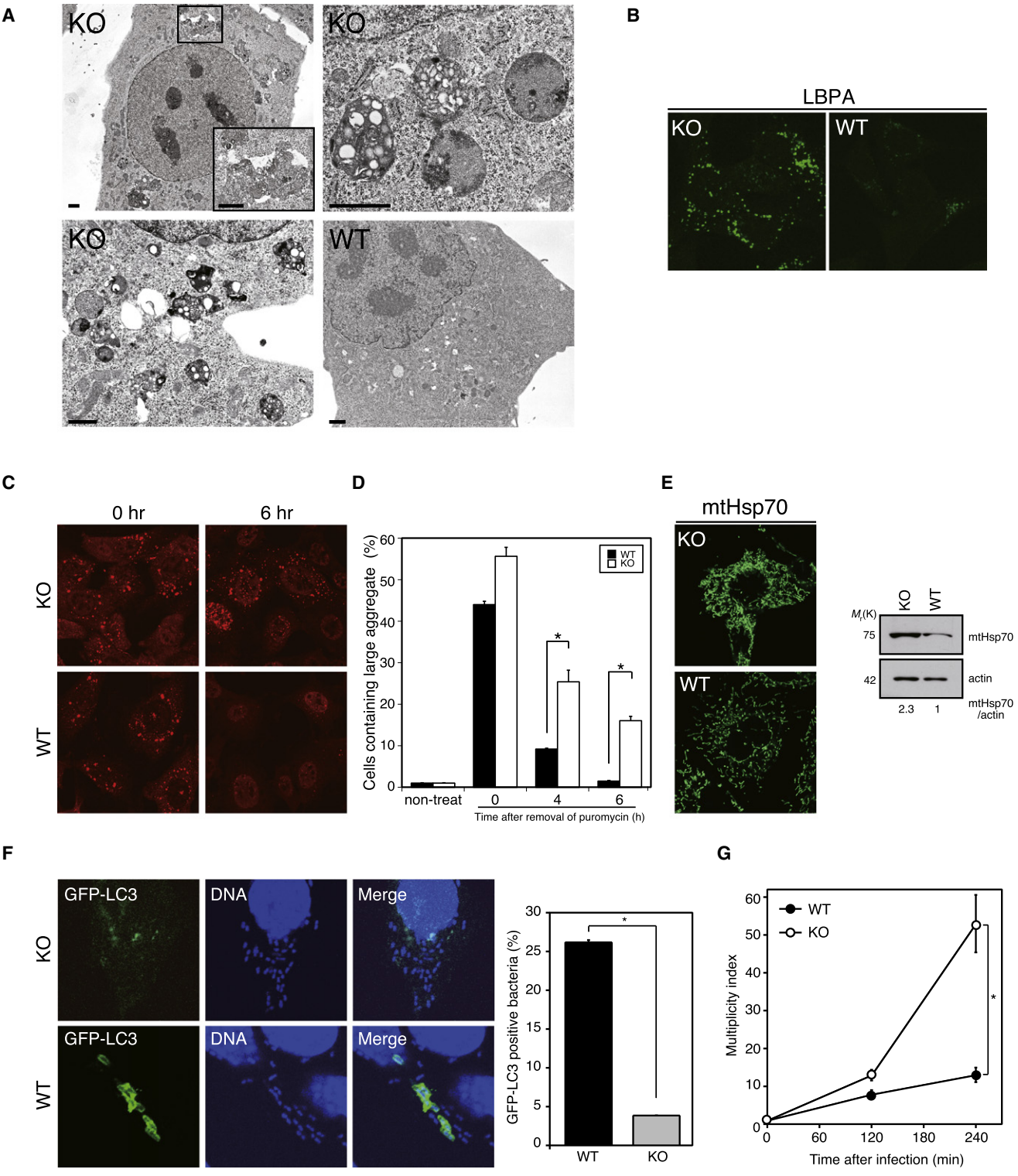

Figure 7. Analysis of MEFs Derived from *tecpr1* Knockout Mice

(A) Tecpr1$^{-/-}$ or Tecpr1$^{+/+}$ MEFs were examined by electron microscopy. Scale bars = 1 μm.

(B) Tecpr1$^{-/-}$ or Tecpr1$^{+/+}$ MEFs were stained with anti-LBPA antibody.

(C and D) Aggregate clearance assay in Tecpr1$^{-/-}$ and Tecpr1$^{+/+}$ MEFs. Aggregates were stained with anti-ubiquitin antibody (C) and the percentage of aggregate-containing cells was calculated (>300 cells, n = 3) (D). Data are the means ± SEM. *p < 0.001.

(E) Tecpr1$^{-/-}$ or Tecpr1$^{+/+}$ MEFs were stained with anti-mtHSP70antibodies (left) and after immunoblotting lysates of Tecpr1$^{-/-}$ or Tecpr1$^{+/+}$ MEFs with anti-mtHSP70 or anti-actin antibodies the mtHSP70/actin ratios were quantified (right).

binding, (3) PI(3)P binding capacity of WIPI-2 is not required for Tecpr1 binding, (4) WIPI-2 was colocalized with Tecpr1 in autophagosomes that targeted *Shigella* Δ*icsB*, and (5) WIPI-2 knockdown reduced the association between Tecpr1 and phagophores that targeted bacteria. Intriguingly, the localization of Tecpr1 to bacteria was dependent on type III PI3K activity and Tecpr1 contains an FRRG motif residing in residues 314–317, which is known as the PI(3)P binding domain conserved in Atg18 family proteins (Polson et al., 2010), but Tecpr1 showed no ability to interact with PI(3)P directly (Figure S3C). Furthermore, the targeting of Tecpr1 to phagophores around *Shigella* Δ*icsB* was much earlier than that of LC3. The results of our study suggested that the PI(3)P associated with phagophores recruited WIPI-2, Tecpr1, and Atg5, in that order and that the recruitment was followed by conjugation between Atg5 and Atg12 and by recruitment of Atg16L1, which leads to LC3 lipidation and results in elongation of phagophores that target bacteria, protein aggregates, and damaged mitochondria (Figure S5). Importantly, this hypothesis is consistent with the accumulation of depolarized mitochondria and misfolded proteins observed in the cytoplasm of the Tecpr1$^{-/-}$ MEFs in this study. Intriguingly, when the *T01H3.2* gene, which encodes the *C. elegans* homolog of Tecpr1, was deleted, abnormal protein aggregates accumulated in the cytosol of worm (WormBase, http://www.wormbase.org). Taken together, these findings further support the biological impact of Tecpr1 involvement in selective autophagy.

The Tecpr1$^{-/-}$ mice produced in this study were born and showed no appreciable phenotypic differences from the wild-type mice in terms of body weight, growth rate, behavior, histological appearance of major organs, and hematological indexes (data not shown). The basal level of autophagy in Tecpr1$^{-/-}$ MEFs was similar to the basal level in Tecpr1$^{+/+}$ MEFs. Nevertheless, the activity of selective autophagy that targets *Shigella* Δ*icsB*, depolarized mitochondria, protein aggregates and MVBs were all greatly reduced in the Tecpr1$^{-/-}$ MEFs, corroborating the involvement of Tecpr1 in selective autophagy. It is also tempting to speculate that the increase in the numbers of MBVs in Tecpr1 knockdown cells and Tecpr1$^{-/-}$ MEFs implies that Tecpr1 is also involved in membrane traffic and endocytic activity.

There is evidence that autophagy is initiated by several distinct pathways, including the ULK1-FIP200-mediated kinase pathway, Beclin-Vps34-mediated PI(3)P pathway, PI(3)P-WIPI-2-mediated membrane-targeting pathway, and Atg12-Atg5-mediated LC3 lipidation pathway (Nakatogawa et al., 2009; Noda et al., 2010; Noda and Yoshimori, 2009; Simonsen and Tooze, 2009), although the mechanism by which Atg5 participates in recruiting autophagy targets to phagophores in the latter two pathways remains elusive in comparison with the mechanisms in the first two pathways. Our findings that Tecpr1 activity is linked to the autophagic machinery, Atg5, and WIPI-2, provide insight into understanding the mechanism by which macromolecular targets, such as bacterial pathogens that have intruded into the cytoplasm, damaged organelles, and protein aggregates are sequestered during the process of selective autophagy (Deretic, 2010b, 2011). We assume that selective autophagy that targets large substrates such as bacterium via the WIPI-2-Tecpr1-Atg5 pathway may require a rapid and bulky elongation of the phagophore membrane and that Tecpr1 may act as an adaptor protein between the autophagy cargo proteins and phagophore and facilitate acceleration of Atg12-Atg5 conjugation for rapid and bulky autophagosome formation. Because the Tecpr1$^{-/-}$ MEFs in our study showed partial decrease in the basal level of autophagy activity, it is tempting to speculate that there is some redundancy of Tecpr1 or some adaptation in Tecpr1$^{-/-}$ MEFs and that some as-yet uncharacterized factor(s) may compensate for the absence of Tecpr1 activity in basal autophagy in Tecpr1$^{-/-}$ MEFs. Indeed, Filimonenko et al. have recently reported that autophagy-linked FYVE protein (ALFY), which has the ability to bind to p62, Atg5, and PI(3)P, plays a pivotal role in selective autophagy for the removal of toxic aggregates in concert with the Ub-p62-LC3 pathway (Clausen et al., 2010; Filimonenko et al., 2010; Simonsen et al., 2004). Thus, Tecpr1 and ALFY may act in the same pathway or in parallel in selective autophagy for aggregate protein. Involvement of ALFY with *Shigella* is unlikely, because the autophagic pathway is Ub independent, while Tecpr1 and ALFY may work together in aggresomes and mitophagy.

In summary, there is evidence that mammalian cells deploy several pathways in selective autophagy that targets bacteria, including a Ub-p62-dependent pathway, a Ub-NDP52-dependent pathway, and a diacylglycerol-dependent pathway. Our discovery of a WIPI-2-Tecpr1-Atg5-dependent pathway gives insight into understanding the mechanism by which a host-defense system senses bacterial pathogens and it may prove useful in identifying therapeutic targets for controlling both autophagy-associated diseases and microbial infection.

EXPERIMENTAL PROCEDURES

Bacterial Strains

Shigella flexneri strain YSH6000 was used as the wild-type strain and its derivatives were constructed and cultured as previously described (Ogawa et al., 2003, 2005). *S. typhimurium* strain SB300 and *Streptococcus pyogenes* (GAS) strain JRS4 were cultured as previously described (Birmingham and Brumell, 2009; Nakagawa et al., 2004; Ogawa et al., 2009). pBRΔtp-DsRed T3_S4T (Sörensen et al., 2003) was transfected into bacteria to visualize living bacteria.

In Vitro Atg12-Atg5 Conjugation Assay

An in vitro Atg12-Atg5 conjugation assay was performed as previously described (Shao et al., 2007) with some modifications. A 40 μl reaction mixture containing reaction buffer (50 mM Tris-HCl [pH 8.0], 100 mM NaCl, 2 mM DTT, 1 mM ATP, and 1 mM $MgCl_2$), 1 μM His-Atg7, 1 μM Atg10, 1 μM MBP-Atg12, and 1 μM Atg5 purified from *Escherichia coli* in the presence of 1 μM MBP-Tecpr1 or MBP was incubated at 30°C for 1 hr and the reaction was stopped by the addition of 2 × Laemmli sample buffer. The Atg12-Atg5 level was determined by immunoblotting with an anti-Atg5 antibody.

(F) Tecpr1$^{+/+}$ or Tecpr1$^{-/-}$ MEFs stably expressing GFP-LC3 were infected with *Shigella* Δ*icsB* and 2 hr later the number of GFP-LC3-positive bacteria was counted (>500 bacteria, n = 3). Data are the means ± SEM. *p < 0.001.
(G) Tecpr1$^{-/-}$ or Tecpr1$^{+/+}$ MEFs were infected with *Shigella* Δ*icsB* and intracellular bacterial growth was determined by cfu (n = 3). Data are the means ± SEM. *p < 0.001.

Aggregate Clearance Assay

Aggregate formation was induced by treatment with 5 μg/ml puromycin for 4 hr. After washing out the puromycin, the cells were incubated for 4 hr or 6 hr. The cells were then fixed and stained with an anti-ubiquitin antibody (Huang et al., 2011).

Flow Cytometric Analyses

The total mass of the mitochondria or mass of polarized healthy mitochondria was assayed by measuring the fluorescence level after staining with MitoTracker Green FM or MitoTracker Red CMXRos (Invitrogen) at 100 nM for 30 min at 37°C. As a negative control, cells were incubated for 2 hr with DMEM and FCS containing 10 μM CCCP before MitoTracker staining. The cells were then washed with PBS three times, trypsinized, and resuspended in DMEM containing 10% FCS for FACS analysis by using FACSAria II (BD) (Tal et al., 2009).

SUPPLEMENTAL INFORMATION

Supplemental Information includes five figures and Supplemental Experimental Procedures and can be found with this article online at doi:10.1016/j.chom.2011.04.010.

ACKNOWLEDGMENTS

We thank O. Igarashi for cell sorting of GFP-fused protein-expressing cells. We thank the members of the Sasakawa Laboratory. This work was supported by a Grant-in-Aid for Young Scientists (B) (21790413); for Scientific Research (B) (20390123) and (S) (20229006); for Exploratory Research (20659067); for Scientific Research on Priority Areas (18073003); for Japan Society for the Promotion of Science-Centre National de la Recherche Scientifique joint research project; and for the Japan Initiative for Global Research Network on Infectious Diseases from the Ministry of Education, Culture, Sports, Science and Technology (MEXT). This work was supported by grants from the Naito Foundation, the Waksman Foundation of Japan Inc., and the Yakult Bio-Science Foundation. The work of J.-M.R. and M.K. was supported by Centre National de la Recherche Scientifique, Université de Strasbourg, grants from L'Agence Nationale de la Recherche (Drosovir ANR-09-MIEN-007), Fondation pour la Recherche Médicale (DEQ 20090515422), and The European Research Council (Immunodroso2009-AdG-20090506).

Received: February 15, 2011
Revised: April 9, 2011
Accepted: April 27, 2011
Published: May 18, 2011

REFERENCES

Ashida, H., Ogawa, M., Mimuro, H., and Sasakawa, C. (2009). *Shigella* infection of intestinal epithelium and circumvention of the host innate defense system. Curr. Top. Microbiol. Immunol. *337*, 231–255.

Behrends, C., Sowa, M.E., Gygi, S.P., and Harper, J.W. (2010). Network organization of the human autophagy system. Nature *466*, 68–76.

Birmingham, C.L., and Brumell, J.H. (2009). Methods to monitor autophagy of *Salmonella* enterica serovar Typhimurium. Methods Enzymol. *452*, 325–343.

Birmingham, C.L., Smith, A.C., Bakowski, M.A., Yoshimori, T., and Brumell, J.H. (2006). Autophagy controls *Salmonella* infection in response to damage to the *Salmonella*-containing vacuole. J. Biol. Chem. *281*, 11374–11383.

Cemma, M., Kim, P.K., and Brumell, J.H. (2011). The ubiquitin-binding adaptor proteins p62/SQSTM1 and NDP52 are recruited independently to bacteria-associated microdomains to target Salmonella to the autophagy pathway. Autophagy *7*, 22–26.

Clausen, T.H., Lamark, T., Isakson, P., Finley, K., Larsen, K.B., Brech, A., Øvervatn, A., Stenmark, H., Bjørkøy, G., Simonsen, A., and Johansen, T. (2010). p62/SQSTM1 and ALFY interact to facilitate the formation of p62 bodies/ALIS and their degradation by autophagy. Autophagy *6*, 330–344.

Deretic, V. (2010a). Autophagy in infection. Curr. Opin. Cell Biol. *22*, 252–262.

Deretic, V. (2010b). Autophagy of intracellular microbes and mitochondria: two sides of the same coin? F1000 Biol Rep *2*, 45.

Deretic, V. (2011). Thematic issue on how autophagosomes find their targets. Autophagy *7*.

Deretic, V., and Levine, B. (2009). Autophagy, immunity, and microbial adaptations. Cell Host Microbe *5*, 527–549.

Dupont, N., Lacas-Gervais, S., Bertout, J., Paz, I., Freche, B., Van Nhieu, G.T., van der Goot, F.G., Sansonetti, P.J., and Lafont, F. (2009). *Shigella* phagocytic vacuolar membrane remnants participate in the cellular response to pathogen invasion and are regulated by autophagy. Cell Host Microbe *6*, 137–149.

Filimonenko, M., Isakson, P., Finley, K.D., Anderson, M., Jeong, H., Melia, T.J., Bartlett, B.J., Myers, K.M., Birkeland, H.C., Lamark, T., et al. (2010). The selective macroautophagic degradation of aggregated proteins requires the PI3P-binding protein Alfy. Mol. Cell *38*, 265–279.

Fu, L., Gao, Y.S., Tousson, A., Shah, A., Chen, T.L., Vertel, B.M., and Sztul, E. (2005). Nuclear aggresomes form by fusion of PML-associated aggregates. Mol. Biol. Cell *16*, 4905–4917.

Fujita, N., Itoh, T., Omori, H., Fukuda, M., Noda, T., and Yoshimori, T. (2008). The Atg16L complex specifies the site of LC3 lipidation for membrane biogenesis in autophagy. Mol. Biol. Cell *19*, 2092–2100.

Gutierrez, M.G., Saka, H.A., Chinen, I., Zoppino, F.C., Yoshimori, T., Bocco, J.L., and Colombo, M.I. (2007). Protective role of autophagy against Vibrio cholerae cytolysin, a pore-forming toxin from V. cholerae. Proc. Natl. Acad. Sci. USA *104*, 1829–1834.

Huang, J., Canadien, V., Lam, G.Y., Steinberg, B.E., Dinauer, M.C., Magalhaes, M.A., Glogauer, M., Grinstein, S., and Brumell, J.H. (2009). Activation of antibacterial autophagy by NADPH oxidases. Proc. Natl. Acad. Sci. USA *106*, 6226–6231.

Huang, J., Birmingham, C.L., Shahnazari, S., Shiu, J., Zheng, Y.T., Smith, A.C., Campellone, K.G., Heo, W.D., Gruenheid, S., Meyer, T., et al. (2011). Antibacterial autophagy occurs at PI(3)P-enriched domains of the endoplasmic reticulum and requires Rab1 GTPase. Autophagy *7*, 17–26.

Jeynov, B., Lay, D., Schmidt, F., Tahirovic, S., and Just, W.W. (2006). Phosphoinositide synthesis and degradation in isolated rat liver peroxisomes. FEBS Lett. *580*, 5917–5924.

Johansen, T., and Lamark, T. (2011). Selective autophagy mediated by autophagic adapter proteins. Autophagy *7*.

Klionsky, D.J., Abeliovich, H., Agostinis, P., Agrawal, D.K., Aliev, G., Askew, D.S., Baba, M., Baehrecke, E.H., Bahr, B.A., Ballabio, A., et al. (2008). Guidelines for the use and interpretation of assays for monitoring autophagy in higher eukaryotes. Autophagy *4*, 151–175.

Komatsu, M., and Ichimura, Y. (2010). Selective autophagy regulates various cellular functions. Genes Cells *15*, 923–933.

Low, D.H., Ang, Z., Yuan, Q., Frecer, V., Ho, B., Chen, J., and Ding, J.L. (2009). A novel human tectonin protein with multivalent beta-propeller folds interacts with ficolin and binds bacterial LPS. PLoS ONE *4*, e6260.

Low, D.H., Frecer, V., Le Saux, A., Srinivasan, G.A., Ho, B., Chen, J., and Ding, J.L. (2010). Molecular interfaces of the galactose-binding protein Tectonin domains in host-pathogen interaction. J. Biol. Chem. *285*, 9898–9907.

Matsushita, M., Suzuki, N.N., Obara, K., Fujioka, Y., Ohsumi, Y., and Inagaki, F. (2007). Structure of Atg5.Atg16, a complex essential for autophagy. J. Biol. Chem. *282*, 6763–6772.

Mizushima, N., Noda, T., Yoshimori, T., Tanaka, Y., Ishii, T., George, M.D., Klionsky, D.J., Ohsumi, M., and Ohsumi, Y. (1998). A protein conjugation system essential for autophagy. Nature *395*, 395–398.

Mizushima, N., Kuma, A., Kobayashi, Y., Yamamoto, A., Matsubae, M., Takao, T., Natsume, T., Ohsumi, Y., and Yoshimori, T. (2003). Mouse Apg16L, a novel WD-repeat protein, targets to the autophagic isolation membrane with the Apg12-Apg5 conjugate. J. Cell Sci. *116*, 1679–1688.

Nakagawa, I., Amano, A., Mizushima, N., Yamamoto, A., Yamaguchi, H., Kamimoto, T., Nara, A., Funao, J., Nakata, M., Tsuda, K., et al. (2004). Autophagy defends cells against invading group A *Streptococcus*. Science *306*, 1037–1040.

Nakatogawa, H., Suzuki, K., Kamada, Y., and Ohsumi, Y. (2009). Dynamics and diversity in autophagy mechanisms: lessons from yeast. Nat. Rev. Mol. Cell Biol. *10*, 458–467.

Narendra, D., Tanaka, A., Suen, D.F., and Youle, R.J. (2008). Parkin is recruited selectively to impaired mitochondria and promotes their autophagy. J. Cell Biol. *183*, 795–803.

Noda, T., and Yoshimori, T. (2009). Molecular basis of canonical and bactericidal autophagy. Int. Immunol. *21*, 1199–1204.

Noda, T., Matsunaga, K., Taguchi-Atarashi, N., and Yoshimori, T. (2010). Regulation of membrane biogenesis in autophagy via PI3P dynamics. Semin. Cell Dev. Biol. *21*, 671–676.

Ogawa, M., Suzuki, T., Tatsuno, I., Abe, H., and Sasakawa, C. (2003). IcsB, secreted via the type III secretion system, is chaperoned by IpgA and required at the post-invasion stage of *Shigella* pathogenicity. Mol. Microbiol. *48*, 913–931.

Ogawa, M., Yoshimori, T., Suzuki, T., Sagara, H., Mizushima, N., and Sasakawa, C. (2005). Escape of intracellular *Shigella* from autophagy. Science *307*, 727–731.

Ogawa, M., Nakagawa, I., Yoshikawa, Y., Hain, T., Chakraborty, T., and Sasakawa, C. (2009). *Streptococcus*-, *Shigella*-, and *Listeria*-induced autophagy. Methods Enzymol. *452*, 363–381.

Patel, P., Harris, R., Geddes, S.M., Strehle, E.M., Watson, J.D., Bashir, R., Bushby, K., Driscoll, P.C., and Keep, N.H. (2008). Solution structure of the inner DysF domain of myoferlin and implications for limb girdle muscular dystrophy type 2b. J. Mol. Biol. *379*, 981–990.

Polson, H.E., de Lartigue, J., Rigden, D.J., Reedijk, M., Urbé, S., Clague, M.J., and Tooze, S.A. (2010). Mammalian Atg18 (WIPI2) localizes to omegasome-anchored phagophores and positively regulates LC3 lipidation. Autophagy *6*, 506–522.

Radoshevich, L., Murrow, L., Chen, N., Fernandez, E., Roy, S., Fung, C., and Debnath, J. (2010). ATG12 conjugation to ATG3 regulates mitochondrial homeostasis and cell death. Cell *142*, 590–600.

Saito, T., Kawabata, S., Hirata, M., and Iwanaga, S. (1995). A novel type of limulus lectin-L6. Purification, primary structure, and antibacterial activity. J. Biol. Chem. *270*, 14493–14499.

Shahnazari, S., Yen, W.L., Birmingham, C.L., Shiu, J., Namolovan, A., Zheng, Y.T., Nakayama, K., Klionsky, D.J., and Brumell, J.H. (2010). A diacylglycerol-dependent signaling pathway contributes to regulation of antibacterial autophagy. Cell Host Microbe *8*, 137–146.

Shao, Y., Gao, Z., Feldman, T., and Jiang, X. (2007). Stimulation of ATG12-ATG5 conjugation by ribonucleic acid. Autophagy *3*, 10–16.

Simonsen, A., and Tooze, S.A. (2009). Coordination of membrane events during autophagy by multiple class III PI3-kinase complexes. J. Cell Biol. *186*, 773–782.

Simonsen, A., Birkeland, H.C., Gillooly, D.J., Mizushima, N., Kuma, A., Yoshimori, T., Slagsvold, T., Brech, A., and Stenmark, H. (2004). Alfy, a novel FYVE-domain-containing protein associated with protein granules and autophagic membranes. J. Cell Sci. *117*, 4239–4251.

Singh, S.B., Ornatowski, W., Vergne, I., Naylor, J., Delgado, M., Roberts, E., Ponpuak, M., Master, S., Pilli, M., White, E., et al. (2010). Human IRGM regulates autophagy and cell-autonomous immunity functions through mitochondria. Nat. Cell Biol. *12*, 1154–1165.

Sörensen, M., Lippuner, C., Kaiser, T., Misslitz, A., Aebischer, T., and Bumann, D. (2003). Rapidly maturing red fluorescent protein variants with strongly enhanced brightness in bacteria. FEBS Lett. *552*, 110–114.

Tal, M.C., Sasai, M., Lee, H.K., Yordy, B., Shadel, G.S., and Iwasaki, A. (2009). Absence of autophagy results in reactive oxygen species-dependent amplification of RLR signaling. Proc. Natl. Acad. Sci. USA *106*, 2770–2775.

Travassos, L.H., Carneiro, L.A., Ramjeet, M., Hussey, S., Kim, Y.G., Magalhães, J.G., Yuan, L., Soares, F., Chea, E., Le Bourhis, L., et al. (2010). Nod1 and Nod2 direct autophagy by recruiting ATG16L1 to the plasma membrane at the site of bacterial entry. Nat. Immunol. *11*, 55–62.

Viala, J.P., Mochegova, S.N., Meyer-Morse, N., and Portnoy, D.A. (2008). A bacterial pore-forming toxin forms aggregates in cells that resemble those associated with neurodegenerative diseases. Cell. Microbiol. *10*, 985–993.